Journal of Materials Chemistry C

Accepted Manuscript

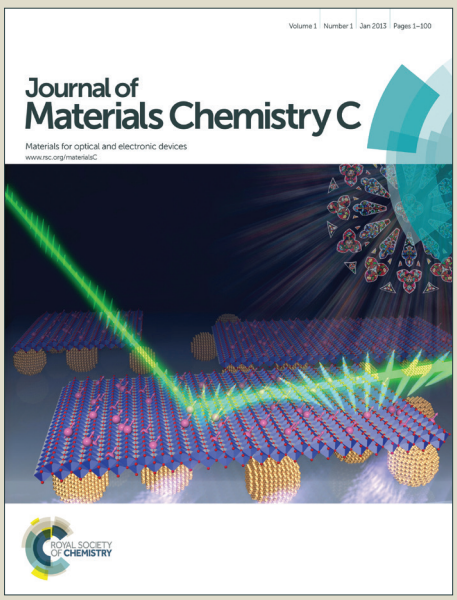

ROYAL SOCIETY OF CHEMISTRY

www.rsc.org/materialsC

Table of Content

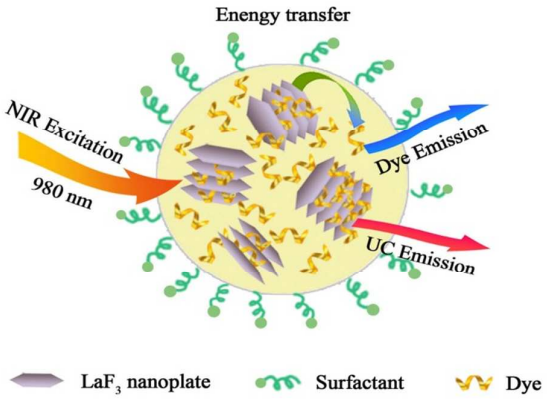

Mesoporous colloidal spheres consisting of LaF_3:Yb,Er/Tm nanoplates are developed, showing tunable upconversion emissions under NIR excitation through dye loading.

Journal Name

RSCPublishing

ARTICLE

Self-assembly of LaF_3:Yb,Er/Tm Nanoplates into Colloidal Spheres and Tailoring Their Upconversion Emissions with Fluorescent Dyes

Cite this: DOI: 10.1039/x0xx00000x

Received 00th January 2012,
Accepted 00th January 2012

DOI: 10.1039/x0xx00000x

www.rsc.org/

Longyi Bao,[ab] Huiling You,[ab] Limin Wang,[c] Lei Li,[a] Ru Qiao,[a] Yong Zhang,[a] Yijun Zhong,[a] Yujie Xiong[c] and Zhengquan Li*[ab]

Colloidal nanoparticles clusters (CNCs) of LaF_3 nanoplates are developed with an emulsion method. Owing to its highly anisotropic shape, these nanoplates can be assembled into spherical particles with various assembly patterns. Investigation on the formation mechanism suggests that two kinds of surfactants, one from the surface of nanocrystals and one from the emulsion, play important roles in directing the assembly patterns of these nanoplates. After doped with lanthanide ions, LaF_3:Yb,Er/Tm CNCs after assembly can show enhanced upconversion fluorescence than their counterparts in a free-standing form. Through loading fluorescent dyes in mesoporous pores of these LaF_3 CNCs, one can finely tune their upconversion emissions through the FRET process.

1. Introduction

In the past decades, significant advances have been made in the synthesis of high-quality nanoparticles with controlled sizes, shapes, compositions, and surface properties. Recently, research efforts have been directed towards the development of secondary structures of colloidal nanoparticles.[1-2] Colloidal nanoparticles clusters (CNCs) with a secondary structure not only allow the combination of properties of individual nanoparticles but also take advantage of the interactions between neighboring nanoparticles which can result in new properties.[2-5] For examples, CNCs assembled from quantum dots can provide stronger signals in biological imaging;[1] CNCs consisting of superparamagnetic nanoparticles show higher saturated magnetization and enhance their applications in separation, targeted delivery and magnetic resonance imaging (MRI);[6-7] CNCs of plasmonic nanoparticles can induce near field electromagnetic coupling and create 'hot spots' that can significantly enhance the Raman signals from analytes.[8-10] Stimulated by these interesting properties, development of robust approaches toward new CNC structures and explore their unique properties are of great importance.

Despite that a few CNCs can be directly obtained by one-step thermolysis or solvothermal technique, evaporation-induced self-assembly of pre-synthesized nanoparticles is a powerful route to attain CNCs with satisfied dimension and uniformity.[1-2] Through confining the nanoparticles in an oil-in-water emulsion, one can acquire CNCs in three-dimension (3D) by evaporating the oil-phase in which the nanoparticles have been dispersed. This assembly strategy has the advantage of fast, cheap, flexible and regardless of the types of nanoparticles. Bai and Li *et al* first demonstrated this assembly process and utilized it to many CNC structures such as $BaCrO_4$, CdS, Fe_3O_4, Ag_2Se, etc.[4] Yin and co-workers pioneered the synthesis of TiO_2 CNCs with mesoporous structures.[11] Cao *et al* developed a modified strategy to prepare ordered packing CNCs of Fe_3O_4 nanoparticles.[12-13] This method can also be applied to other types of CNCs by modifying the surfactants and/or solvents.[1-2] In most successful cases, the primary nanoparticles are limited in small nanocrystals with a diameter below 10 nm. Once the size of nanoparticles increases to some extent (e.g., above 10 nm), uniform and regular CNCs can only be achieved on some spherical or analogous nanoparticles such as nanopolyhedrons.[14-15] Up to date, there are few reports referring to the self-assembled CNCs which are composed of anisotropic nanoparticles with one dimension above 30 nm. Exploring appropriate approaches for assembly of anisotropic nanoparticles and investigating their novel properties are new challenging tasks confronted by materials scientists.

In this work, we demonstrate the self-assembly of LaF_3 nanoplates with a highly anisotropic shape and exploration of their intriguing fluorescent properties. In our previous work, we have developed a facile method to synthesize LaF_3 with various shapes and LaF_3 nanoplates with a length of 36 nm and a thickness of only 4 nm could be obtained.[16] Nanoparticles with such a high length-to-thickness ratio provide us a good opportunity to study its unique self-assembly mechanism. Unlike previous developed CNC structures, the CNCs

consisting of LaF_3 nanoplates display various assembly patterns among the assembled particles due to their anisotropic shapes. Two kinds of surfactants, one from the surface of nanocrystals and one from the emulsion, have been found to play different roles in the assembly of these nanoplates, resulting in various kinds of organizations of nanoplates in the LaF_3 CNCs. On the other hand, the CNCs packed by primary nanocrystals exhibit mesoporous structures which provide us a good chance to load various agents inside the LaF_3 CNCs. Here we also present a strategy to finely tune the fluorescent emissions of luminescent nanocrystals through loading suitable dyes inside the CNCs. As a proof-of-concept work, upconversion (UC) LaF_3:Yb,Er/Tm CNCs with single-band emission or targeted emissions have both been achieved by this strategy based on the fluorescence resonant energy transfer (FRET) process. This work may shed some new lights on the self-assembly of anisotropic nanocrystals and creating functional phosphors with controllable fluorescence.

2. Experimental Section

2.1 Synthesis of thin LaF_3 nanoplates

LaF_3 nanoplates were synthesized according to a protocol we developed recently.[16] In a typical synthesis, 1 mmol $LaCl_3$ was dissolved in a mixed solution of 4 mL oleic acid (OA) and 16 mL octadecene (ODE) by heating at 160 ºC. Once the $LaCl_3$ was completely dissolved, forming a yellow transparent solution, the solution was cooled down to room temperature. Meanwhile, 1.5 mmol NaOH and 3 mmol NH_4F were dissolved in 5 mL methanol in a plastic tube by sonication. To initiate the reaction, the prepared methanol solution was slowly added in above ODE solution under vigorous stirring. The mixed solution was then heated to 80 ºC to evaporate the methanol and degassed at 100 ºC for 20 min. Subsequently, the solution was slowly heated to 280 ºC and maintained at this temperature for 1 h under argon protection. Once the solution was naturally cooled down to room temperature, double volume of ethanol was poured into the solution. The LaF_3 nanoplates were collected from the solution by centrifuge at a speed of 6 000 rpm. After being washed by chloroform and acetone twice, these nanoplates were finally dispersed in 10 mL chloroform. Lanthanide-doped LaF_3 nanoplates (i.e., LaF_3:18%Yb, 2%Er and LaF_3:18%Yb, 0.5%Tm) were also obtained through the similar process by introducing a certain amount of other lanthanide chlorides (i.e., $YbCl_3$, $ErCl_3$ or $TmCl_3$) along with $LaCl_3$ at the first step.

2.2 Self-assembly of LaF_3 nanoplates into CNCs

The emulsion was formed by mixing a certain ratio of chloroform, cetyltrimethylammonium bromide (CTAB) and water which acted as oil-phase, surfactant and aqueous phase, respectively. In a typical experiment, 0.2 mL of LaF_3 nanoplates in chloroform and 0.2 g CTAB were mixed with 30 mL deionized (DI) water. After being sonicated for 10 min, the mixed solution were put in a water bath (set at 40 ºC) and magnetically stirred for 8 h. During this process, the chloroform was slowly evaporated, leading to the condensation of LaF_3 nanoplates in DI water. Final products (i.e., LaF_3 CNCs) were collected from the aqueous solution by centrifuging at a speed of 6 000 rpm.

2.3 Loading dyes in LaF_3 CNCs

The synthetic process to dye-loaded LaF_3 CNCs is similar to that of pure LaF_3 CNCs except that a few dye molecules (i.e., Nile red and Coumarin 6) were added in the chloroform solution before the formation of an emulsion. In a typical synthesis, 1 μmol Nile red (or 1 μmol Coumarin 6) was added in the chloroform solution of LaF_3 nanoplates, prior to being added in 30 mL DI water which contains 0.2 g CTAB. The mixed solution was sonicated for 10 min and then magnetically stirred in a water bath (40 ºC) for 4 h. Finally, the products were collected by centrifuging and washed with DI water twice.

2.4 Characterizations

Low-magnification transmission electron microscopy (TEM) images were taken on a Hitachi H-7650 TEM which was operated at 110 kV. High-resolution TEM images were recorded on a JEOL 2010F TEM operated at 220 kV. The TEM samples were prepared by dropping a suspension of nanocrystals on a polymer-film coated copper grid. UC spectra of samples were acquired on an Edinburgh FLS920 steady-state/time-resolved spectrometer equipped with a commercial 980 nm NIR laser.

3. Results and Discussion

3.1 Characterizations of LaF_3 nanoplates and assembly strategy

Fig. 1A gives a typical TEM image of LaF_3 nanoplates prepared according to the protocol we have previously developed.[16] These nanoplates were synthesized with surfactant OA as capping ligands and thus they possessed a hydrophobic surface.[16-17] When the particle solution (0.05 M) was dropped

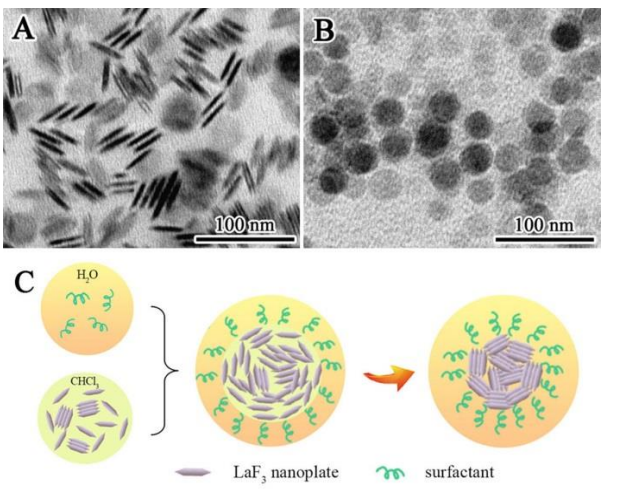

Fig. 1 (A) and (B) are TEM images of prepared LaF_3 nanoplates, showing their side and front planes respectively; (C) is a schematic to illustrate the self-assembly strategy of LaF_3 nanoplates.

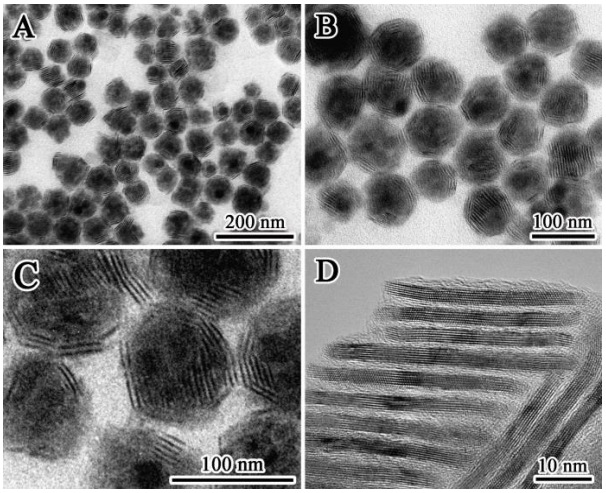

Fig. 2 (A), (B) and (C) are TEM images of the prepared CNCs consisting of LaF_3 nanoplates at different magnifications; (D) is a high-resolution TEM image of LaF_3 CNC showing the organization of nanoplates.

under a copper grid, many LaF_3 nanoplates stood upright with their lateral planes, exhibiting a slim rice appearance. Such an orientation of nanoplates is ascribed to van der Waals' interactions between the hydrophobic tails of OA molecules attached on the nanoplates.[18] If the particle solution was diluted (0.001 M) and slowly dried on a copper grid, most of the nanoplates prefer to lie down with their flat planes in order to reduce the surface energy (Fig. 1B).[16, 18] Average diameter of these nanoplates is about 36 nm while their thickness is just 4 nm. Obviously, these prepared LaF_3 nanoplates have a highly anisotropic shape due to its high length-to-thickness ratio.

To induce self-assembly of these LaF_3 nanoplates into CNCs, we adapted an emulsion-based evaporation strategy which is illustrated in Fig. 1C. In order to build an oil-in-water emulsion, surfactant CTAB was employed as an emulsifier in a mixed solution of water and chloroform. LaF_3 nanoplates were initially dispersed in chloroform before the formation of emulsion. Through vigorous stirring and ultrasonic treatment, color of the mixed solution was changed from milky to transparent, indicating that uniform oil-in-water droplets have been formed. When the emulsion was aged in a flask under stirring, the oil phase (chloroform) would slowly evaporate. Therefore, the LaF_3 nanoplates were gradually condensed in the residual oil under the assistance of surfactant CTAB. Once the chloroform was completely evaporated, compact CNC spheres consisting of LaF_3 nanoplates were produced in the aqueous solution. At the same time, many CTAB molecules were adsorbed on the surface of LaF_3 CNCs (i.e., the surface of the formed colloidal spheres) (see Fig. S1 and S2), which enabled good water dispersibility of these CNCs. These CNCs can be stabilized in aqueous solution for weeks.

3.2 Morphologies and assembly patterns of LaF_3 CNCs

TEM images of the prepared LaF_3 CNCs at different magnifications are shown in Fig. 2. From the low-magnification

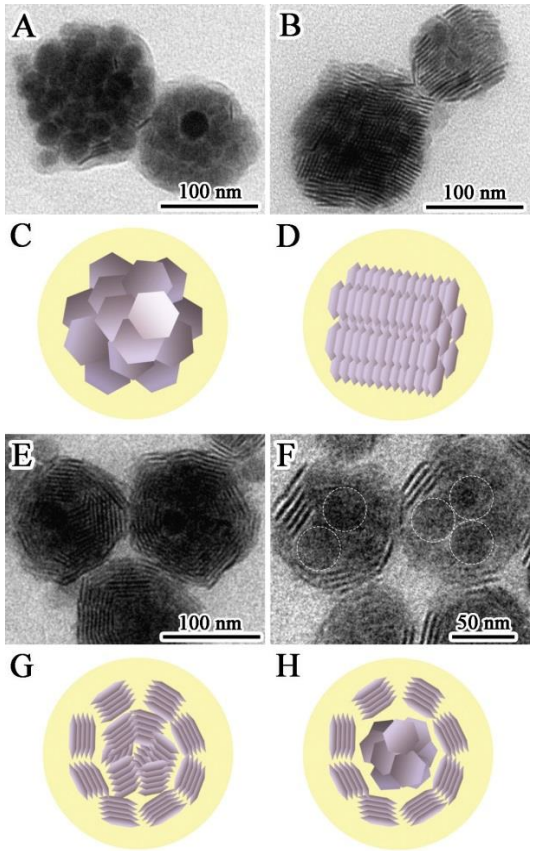

Fig. 3 (A), (B), (E) and (F) are typical TEM images showing the different assembly patterns in the LaF_3 CNCs; (C), (D), (G) and (H) are corresponding schematic diagrams showing the arrangement of nanoplates in different patterns.

image (Fig. 2A), one can see that the products are purely spherical spheres and no free nanoplate is found, suggesting that all LaF_3 nanoplates have been assembled into spheres. These spheres have a diameter of 80-100 nm with a narrow size distribution. Magnifying the TEM images (see Fig. 2B and 2C), one can see many distinct stripes in each sphere. Length and thickness of these stripes are consistent with those of the LaF_3 nanoplates, implying that each stripe is a single LaF_3 nanoplate. Most LaF_3 nanoplates stand upright with their lateral planes in the spheres, showing a face-to-face assembly pattern. This result is attributed to the fact that such an orientation can greatly reduce their surface area. Between two adjacent LaF_3 nanoplates (see Fig. 1D), there is a small gap around 3.5 nm. The distance is closed to that of two assembled layers of OA molecules, implying that the surface-attached OA on LaF_3 nanoplates are also responsible to the face-to-face assembly pattern.

Detailed assembly patterns of LaF_3 nanoplates inside these CNCs are further investigated. Interestingly, we find that each CNC sphere is constituted by a few plate clusters, suggesting that the LaF_3 nanoplates were initially assembled to clusters which were sequentially integrated into individual spheres. In each cluster, orientation of LaF_3 nanoplates is consistent and the nanoplates are organized with a face-to-face pattern. In order to reach an overall spherical appearance, orientations

between different clusters are varied from case to case. Fig. 3 gives four typical TEM images to display various assembly patterns of these LaF_3 nanoplates. Corresponding schematics are also depicted to illustrate the inner organizations of these nanoplates. From these images, one can see that the inner structures of LaF_3 CNCs are much different from previously developed CNCs consisting of spherical or analogous nanocrystals.[1,4] Specifically, the LaF_3 CNCs have a secondary assembly into spheres which follows a preliminary assembly of LaF_3 nanoplates into plate clusters. Both kinds of assembles is attributed to two kinds of surfactants exist in the system. In the preliminary assembly, formation of plate clusters is driven by the surface-attached OA molecules when the hydrophobic nanoplates encounter a polar solvent (i.e., water in the emulsion). In the secondary assembly, pre-formed clusters are guided by the CTAB molecules for maintaining a spherical geometry at the water/oil interface of the emulsion.

3.3 Influence of surfactants

In our control experiments, it was found that the amount of CTAB has a great effect on the size and uniformity of final spheres. With 1 mg/mL of CTAB or above, only free LaF_3 nanoplates are obtained in the final solution (Fig. 4A). There are no obvious assembled particles under this condition, suggesting that excessive surfactants serve only as surface-modify agents to transfer hydrophobic LaF_3 nanoplates to be hydrophilic ones. This phase-transfer is realized through van de Walls interaction between long tails of OA and CATB, leaving hydrophilic heads of the latter pointing outward. This result is consistent with previous researches using CTAB as a phase-transfer agent.[19-20] When the CTAB concentration is reduced (e.g., 0.8 mg/mL), small CNCs consisting of only few LaF_3 nanoplates appear (Fig. 4B). But these particles have a relatively large size-distribution. As the CTAB concentration decreases to some extent (e.g., 0.5 mg/mL and 0.2 mg/mL), sizes of these spheres increase and their uniformities become greatly improved (see Fig. 4C and 4D). Uniform LaF_3 CNCs with a regular spherical shape can be obtained in this range of CTAB concentration. If one further decreases the CTAB concentration (e.g., 0.1 mg/mL and 0.05 mg/mL), the spheres become adhesive with a poor uniformity although their sizes still increase (see Fig. 4E and 4F). Above morphological change of samples can be understood from the effect of CTAB concentration on the oil droplets of an emulsion. Specifically, the sizes of oil droplets increase with the decrease in CTAB concentration. Uniform and regular spherical droplets are usually formed with a certain ratio of surfactants to oil.[21-22] Above results also indicate that assistance of CTAB is responsible for the spherical morphology of the LaF_3 CNCs.

Other surfactants with different charge or chain length were also applied in the self-assembly of LaF_3 nanoplates. As displayed in Fig. 5, spherical LaF_3 CNCs have been obtained in all the cases but size and uniformity of products are different. With short alkyl-chain surfactants such as sodium lauryl sulfate (SDS) and Dodecyltrimethylammonium bromide (DTAB), big LaF_3 CNCs with a sticky morphology are obtained (Fig. 5A and 5B). There is no obvious difference between these two products, implying that the charge of surfactants has negligible effect on final samples when the lengths of surfactants are comparable. If sodium dodecylbenzenesulphonate (SDBS) is used as surfactant, dispersibility of the CNCs can be improved while its uniformity is still poor (Fig. 5C). Uniform CNCs structures with a narrow side-distribution are obtained when CTAB is employed (Fig. 5D), suggesting that long chain alkyl group can help to decrease the particle size and improve its uniformity. Above phenomenon can also be interpreted from the stability of an emulsion formed by different surfactants, because surfactants

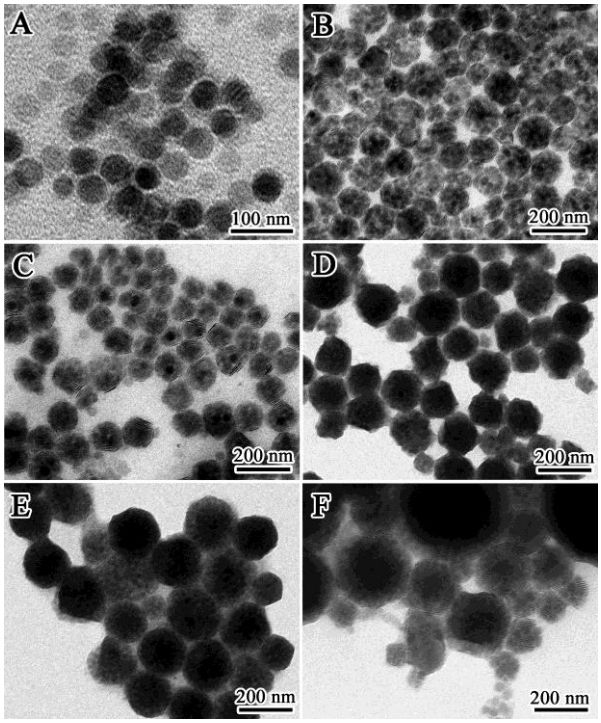

Fig. 4 TEM images of LaF_3 CNCs prepared with different concentrations of CTAB: (A) 1 mg/mL; (B) 0.8 mg/mL; (C) 0.5 mg/mL; (D) 0.2 mg/mL; (E) 0.1 mg/mL; (F) 0.05 mg/mL.

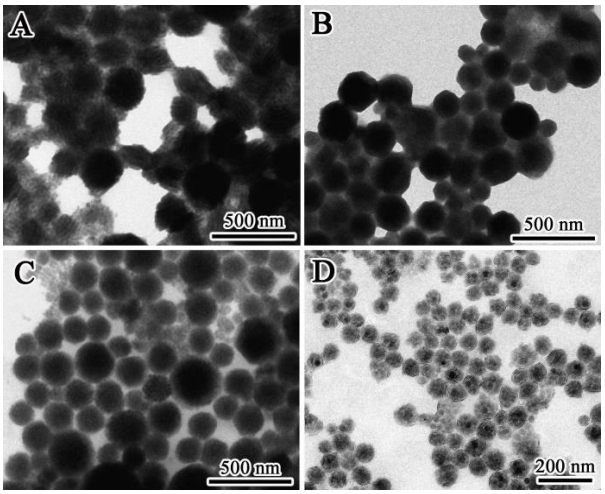

Fig. 5 TEM images of self-assembled LaF_3 CNC prepared with different kinds of surfactants: (A) SDS; (B) DTAB; (C) SDBS; (D) CTAB.

with a long chain or big head can improve the uniformity and stability of an emulsion.[23-24]

3.4 UC Fluorescence of LaF_3:Yb,Er/Tm CNCs

Various lanthanide ions can be doped in the LaF_3 nanoplates during the synthesis and corresponding products can show down- and/or up-conversion emissions depending on the doping ions. In this work, we focus on investigation of UC fluorescence of assembled Ln^{3+}-doped LaF_3 nanoplates in aqueous solution. After co-doped with Yb^{3+} and Er^{3+}, the LaF_3 CNCs display strong UC emissions at 521 nm, 539 nm and 653 nm, owing to the transitions of $^2H_{11/2}$–$^4I_{15/2}$, $^4S_{3/2}$–$^4I1_{5/2}$, and $^4F_{9/2}$–$^4I_{15/2}$ in Er^{3+} ions.[25-26] When Yb^{3+} and Tm^{3+} were co-doped, a strong blue emission at 479 nm appears due to the $^1G_4$–$^3H_6$ transition in Tm^{3+} ions.[27-28] For comparison of UC fluorescence of the nanoplates before and after assembly, we not only prepared assembled LaF_3:Yb,Er/Tm CNCs in water but also synthesized free LaF_3:Yb,Er/Tm nanoplates in aqueous solution using the phase-transfer method aforementioned (see Fig. 6A). As such, fluorescence influence from solvents could be excluded when making a direct comparison between these two kinds of samples based on the same amount of nanoplates. Interestingly, obvious stronger UC fluorescence appears in the assembled samples no matter what kinds of ions are co-doped. This result suggests that rational assembly of LaF_3:Yb,Er/Tm nanoplates is an effective route to preserve their intrinsic fluorescence from the heavy quenching of surrounding solvents (e.g., water), because only a few nanoplates were directly exposed to water in the assembled CNCs. Besides improvement of total fluorescence, these assembled LaF_3 CNCs also have obvious advantages in bioimging application since they can enhance fluorescent signals by locally multiplying the fluorescence at one targeting spot.

3.5 Tailoring UC emissions of LaF_3:Yb,Er/Tm CNCs with dyes

The CNCs are formed by packing primary nanoparticles and lots of small vacancies are created between nanoparticles. As such, the CNCs have a mesoporous structure which enables them many new functions such as drug delivery, bioseparation, and catalyst supports (see Fig. S3).[1-2] For UC phosphors, it is still challenging to finely tune the UC emissions because optimal UC fluorescence is generally attained by doping a certain ratio of Er^{3+}, Tm^{3+} or Ho^{3+} with Yb^{3+} in the host materials.[29-31] Herein, we propose that the CNC structures can provide a facile way to control the UC emissions by loading fluorescent dyes inside their mesoporous pores, based on the FRET process (see Fig. 7A). Under the NIR excitation, LaF_3:Yb,Er/Tm nanoplates in each CNC can emit several intrinsic emissions which can serve as electron donors to excite the loaded dyes to give expectable emissions. For instance, we have loaded Nile red as an electron receptor to finely tune the intensity ratio between the green and red emissions in these LaF_3:Yb,Er CNCs (Fig. 7B). Through controlling the amount of Nile red, the green emission will decrease along with the dye concentration while the red emission gradually increases. This result is attributed to the fact that the green emission has acted

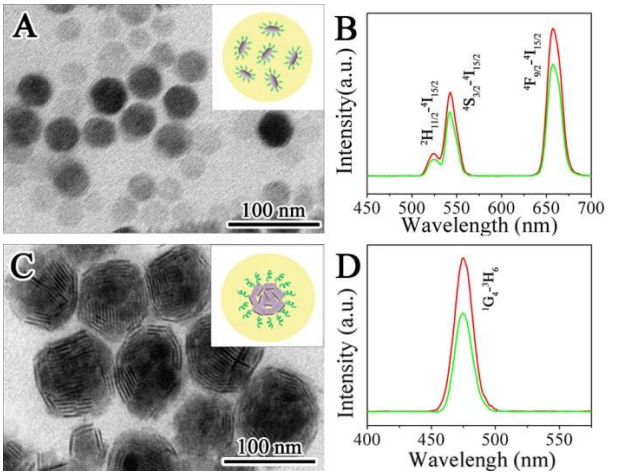

Fig. 6 (A) and (C) are TEM images of LaF_3:Yb,Er nanoplates in the form of free-standing and in the form of self-assembly, respectively. Insets are corresponding schematics of the nanoplates in different forms. (B) and (D) are UC spectra of LaF_3:18%Yb, 2%Er nanoplates and LaF_3:18%Yb, 0.5%Tm nanoplates in different forms, respectively. (Red line: assembly; green line: free-standing)

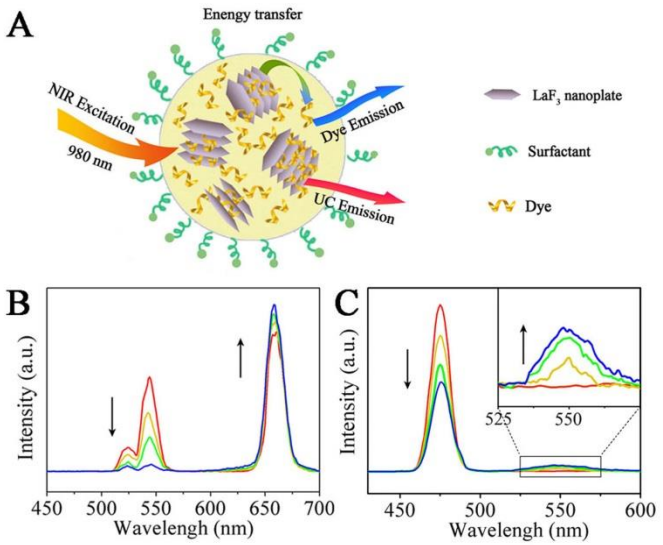

Fig. 7 (A) Schematics of energy transfer process in the dye-loaded LaF_3:Yb,Er/Tm CNCs; (B) UC spectra of LaF_3: 18%Yb, 2%Er CNCs loaded with different amount of Nile red; (C) UC spectra of LaF_3: 18%Yb, 0.5%Tm CNCs loaded with different a amount of Coumarin 6. (Red line: 0.1 μmol; yellow line: 0.2 μmol; green line: 0.3 μmol; blue line: 0.4 μmol)

as an electron donor for Nile red which can emit a red emission whose location matches well with the red emission of LaF_3:Yb,Er nanoplates. Particularly, near single-band red emission can be obtained when the payload of Nile red is above 4 μmol. Single-band UC phosphors can provide better monochromaticity and resolution in biomedical applications, which is a new tread in the development of UC materials.[32] In comparison with the component nanoplates, the loading amount of dyes is very low in these spherical assemblies. The concentrations of loaded dyes can be measured by UV-Vis spectroscopy (see Fig. S4), which turns out to be reproducibly controlled.

Besides tuning the intrinsic UC emissions from a phosphor, new UC emissions can also be realized by loading suitable dyes in these CNCs. If a dye can be excited by the UC emissions from nanoplates and give a different emission, the whole CNC will give a new UC fluorescence upon NIR excitation. Thus, desirable UC emissions can be expected by selecting an appreciate dye in the CNCs. As a proof-of-concept work, we have achieved green emission by loading Coumarin 6 in LaF_3:Yb,Tm nanoplates which originally give a single blue emission prior to dye loading. As shown in Fig. 7C, a green emission at 550 nm comes into being and gradually enhance along with the increase of dye concentration. Based on above strategy, in principle, various UC emissions can be anticipated in these CNCs through loading different dyes. Although the new UC emission is not sufficiently strong at present case, peak intensity can be improved through other approaches such as increasing excitation power or using other dyes with a higher quantum yield.

Based on the similar FRET strategy, many other practical applications can also be initiated by loading suitable fluorescent species in these CNCs. For examples, one can load fluorescence-responsive dyes or ligands in these CNCs for detection of heavy metal ions and enrich them in the mesoporous pores. Drug delivery can also be realized by incorporating fluorescence-responsive drugs inside the CNCs and release them upon NIR irradiation. Above proposed work is under investigation in our group and other promising application is also under pursue.

4. Conclusions

In summary, we have demonstrated a facile emulsion route for self-assembly of LaF_3 nanoplates into CNC structures. The LaF_3 CNCs consisting of anisotropic nanoplates displayed various assembly patterns due to its high thickness-to-length ratio. It was revealed that two types of surfactants can play different roles in directing the assembly of LaF_3 nanoplates. Influence of CTAB concentration and other surfactants on the assembly of LaF_3 nanoplates is also investigated. The LaF_3:Yb,Er/Tm CNCs in aqueous solution shows a better UC fluorescence than free nanoplates at the same concentration. Through the FRET process, we can finely tune the UC emissions of CNCs by loading suitable fluorescent dyes. The developed LaF_3:Yb,Er/Tm CNCs may have great potential in biomedical applications due to their uniform sizes, mesoporous structures and tunable UC emissions.

Acknowledgements

The authors acknowledge financial support from National Nature Science Foundation of China (nos 21273203 and 21201151) and Natural Science Foundation of Zhejiang Province (No. LY12B01001).

Notes and references

[a] Institute of Physical Chemistry, Zhejiang Normal University, Jinhua, Zhejiang 321004, P. R. China.
[b] Department of Materials Physics, Zhejiang Normal University, Jinhua, Zhejiang 321004, P. R. China.
[c] Department of Chemistry, University of Science and Technology of China, Hefei, Anhui 230026, P. R. China.

1. Z. Lu and Y. Yin, *Chem. Soc. Rev.*, 2012, **41**, 6874.
2. Y. Xia and Z. Tang, *Chem. Commun.*, 2012, **48**, 6320.
3. Z. Lu, C. Gao, Q. Zhang, M. Chi, J. Y. Howe and Y. Yin, *Nano Lett.*, 2011, **11**, 3404.
4. F. Bai, D. Wang, Z. Huo, W. Chen, L. Liu, X. Liang, C. Chen, X. Wang, Q. Peng and Y. Li, *Angew. Chem. Int. Ed*., 2007, **46**, 6650.
5. P. Li, Q. Peng and Y. Li, *Adv. Mater.*, 2009, **21**, 1945.
6. J. Ge, Y. Hu, M. Biasini, W. P. Beyermann and Y. Yin, *Angew. Chem. Int. Ed.*, 2007, **46**, 4342.
7. J. Kim, J. Lee, S. Lee, J. Yu, J. Lee, T. G. Park and T. Hyeon, *Adv. Mater*., 2008, **20**, 478.
8. S. Lin, M. Li and E. Dujardin, *Adv. Mater*., 2005, **17**, 2553.
9. S. Nie and S. R. Emory, *Science*, 1997, **275**, 1102.
10. P. Taladriz-Blanco, N. J. Buurma, L. Rodriguez-Lorenzo, J. PerezJuste, L. M. Liz-Marzan and P. Herves, *J. Mater. Chem*., 2011, **21**, 16880.
11. Z. Lu, M. Ye, N. Li, W. Zhong and Y. Yin, *Angew. Chem. Int. Ed.*, 2010, **49**, 1862.
12. J. Zhuang, H. Wu, Y. Yang and Y. C. Cao, *Angew. Chem. Int. Ed.*, 2008, **47**, 2208.
13. J. Zhuang, H. Wu, Y. Yang and Y. C. Cao, *J. Am. Chem. Soc.*, 2007, **129**, 14166.
14. Q. Zhang, X. Wang and Y. Zhu, *J. Mater. Chem*., 2011, **21**, 12132.
15. S. Liang, X. Zhang, Z. Wu, Y. Liu, H. Zhang, H. Sun, H. C. Sun and B. Yang, *CrystEngComm*, 2012, **14**, 3484.
16. L. Bao, Z. Li, Q. Tao, J. Xie, Y. Mei and Y. Xiong, *Nanotechnology*, 2013, **24**, 145604.
17. H. Mai, Y. Zhang, R. Si, Z. Yan, L. Sun, L. You, C. Yan, *J. Am. Chem. Soc*., 2006, **128**, 6426.
18. R. Si, Y. Zhang, L. You and C. Yan, *Angew. Chem. Int. Ed.*, 2005, **44**, 3256.
19. A. Swami, A. Kumar and M. Sastry, *Langmuir*, 2003, **19**, 1168.
20. J. Yang, Y. Deng, Q. Wu, J. Zhou, H. Bao, Q. Li, F. Zhang, F. Li, B. Tu and D. Zhao, *Langmuir*, 2010, **26**, 8850.
21. Y. Qiu, P. Chen and M. Liu, *J. Am. Chem. Soc*. 2010, **132**, 9644.
22. K. Landfester, N. Bechthold, F. Tiarks and M. Antonietti, *Macromolecules*, 1999, **32**, 5222.
23. T. Sottmann, C. Stubenrauch, *in Microemulsion: Background, New Concept, Applications, Perspectives* Vol. 1 (Eds: C. Stubenrauch), Wiley-VCH, Weinheim, Germany **2009**, Ch. 2.
24. D. Das, S. Roy, R. N. Mitra, A. Dasgupta and P. K. Das, *Chem. Eur. J.*, 2005, **11**, 4811.
25. J. W. Stouwdam and F. C. J. M. van Veggel, *Nano Lett.*, 2002, **2**, 733.
26. Z. Q. Li, L. M. Wang, Z. Y. Wang, X. H. Liu and Y. J. Xiong, *J. Phys. Chem. C*, 2011, **115**, 3291.
27. Y. Liu, D. Tu, H. Zhu, R. Li, W. Li and X. Chen, *Adv. Mater.*, 2010, **22**, 3266.
28. H. Guo, Z. Q. Li, H. S. Qian, Y. Hu and I. N. Muhammad, *Nanotechnology*, 2010, **21**, 125602.

29. F. Wang and X. Liu, *Chem. Soc. Rev.*, 2009, **38**, 976.
30. D. K. Chatterjee, M. K. Gnanasammandhan and Y. Zhang, *Small*, 2010, **6**, 2781.
31. C. Li and J. Lin, *J. Mater. Chem.*, 2010, **20**, 6831.
32. J. Wang, F. Wang, C. Wang, Z. Liu and X. Liu, *Angew. Chem. Int. Ed.*, 2011, **50**, 10369.